ACADEMIA ROMÂNĂ
Revue Roumaine de Chimie
http://web.icf.ro/rrch/

Rev. Roum. Chim.,
2017, *62*(2), 181-190

EXPLORATORY INFRARED SPECTROSCOPY STUDY OF ERYTHROCYTES IN CANCER CHEMOTHERAPY**

Mihai GUTU,[a] Mihaela AVADANEI,[b,*] Mihai MARINCA[c] and Cipriana STEFANESCU[b]

[a] Biophysics and Medical Physics Department, Medicine Faculty, "Gr. T. Popa" University of Medicine and Pharmacy, 6, Universitații Str., 700115 Iași, Roumania
[b] "Petru Poni" Institute of Macromolecular Chemistry, 41A Aleea Grigore Ghica Voda, 700487 Iași, Roumania
[c] Regional Oncology Institute, 2-4 Gen. Henri Mathias Berthelot St., 700483 Iași, Roumania

Received September 5, 2016

Structural modifications of human erythrocytes are known to occur in cancer patients, especially those undergoing chemotherapy. Fourier transform infrared spectroscopy (FTIR) is a potentially useful method for detecting these changes. The purpose of this study was to compare the hematological and biochemical parameters with the spectral parameters of a study group (patients with digestive cancer) in respect with a control one, in order to establish the possible relations with chemotherapy-induced anemia (CIA). Specific FTIR marker bands (such as the $\nu_{as}(CH_2)$/ ν(=CH) ratio of the plasmatic membrane) were correlated with the used cytotoxics, the degree of unsaturation/saturation of the membrane fatty acids, the alterations of the hemoglobin molecule and hematological parameters. The spectral features responsible for the group-wise biochemical differences in erythrocytes were tentatively identified from the PCA loading plots, obtained in the same spectral regions.

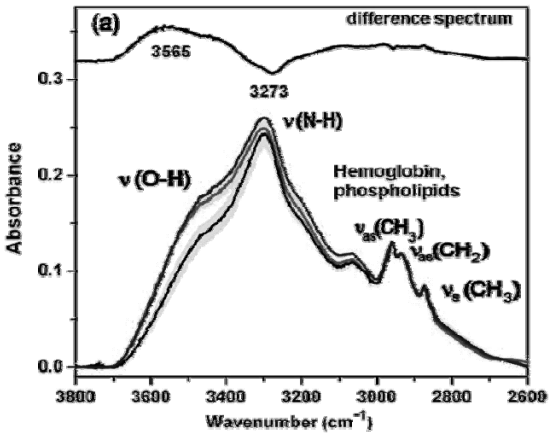

INTRODUCTION

The evaluation of clinical status and biochemical changes is a key factor in treating different pathologies. Thus, medicine is compelled to find methods for modulating the flow of a drug or assessing treatment side effects, in order to maintain an acceptable risk/benefit ratio. The red blood cells possess a great potential to reveal important hints concerning the health status of a person and are a sensitive marker of blood biochemical changes in different pathological situations.[1-10] In various types of cancer, the structure and function of hemoglobin is altered as the result of the oxidative process, during which the so-called "Heinz bodies" could be formed. At the membrane level, particular lipids could be altered by peroxidation, affecting the normal asymmetric structure of the membrane and resulting in its increased rigidity and lysis.[7-10] Studies on cancer patients reported significant changes in the erythrocyte membrane fatty acid distribution and structure.[11-14] The anomalous distribution of the fatty acids in erythrocyte membrane has been monitored through the ratio of saturated/unsaturated fatty acids, which is defined as the saturation index, SI. The relationship between SI and the peroxidation process was used to evaluate the effects of carcinogenesis on erythrocyte membrane.[14-16]

* Corresponding author: mavadanei@icmpp.ro or cipriana.stefanescu@yahoo.com
** Supporting information on http://web.icf.ro/rrch or http: //revroum.lew.ro

Chemotherapy itself induces structural changes in erythrocyte membrane and hemoglobin, due to the direct interaction between the drug molecules and the components of the erythrocytes.[17-23] Generally, the toxicity of the chemotherapeutic agents is correlated to the molecular mechanism by which the antitumor activity is performed. The erythrocytes may act only as drug carriers, and even in this case either the membrane[17-19] or hemoglobin might experience serious structural alterations.[20-23]

Vibrational spectroscopy is now largely employed in characterization of tissues, cell lines and RBCs in various pathologies because it is non-invasive, label-free, and cost-effective. Infrared spectroscopy is known to probe the structure, dynamics and functions of red blood cells[24-31] and can provide direct insight into the biochemical mechanism responsible for their abnormal functioning under the influence of disease and/or cytotoxics. The structural modifications of erythrocytes can be followed at both the membrane and cytoplasmic levels.

This paper reports the results of an exploratory study using Fourier transform infrared spectroscopy (FTIR) to monitor the effects of cancer and chemotherapy on the human erythrocyte structure. Due to its increased incidence and the relative uniformity of the chemotherapy regimens used, the patients with digestive cancer were investigated. The purpose of the study was to determine to what extent the FTIR characteristics could be specific for cancer patients undergoing chemotherapy. A secondary objective was to evaluate the feasibility and reproducibility of the measurements, and their possible future clinical applications.

EXPERIMENTAL SECTION

1. Blood Specimen Collection and Processing

The blood samples for the case studies were obtained from 15 male patients diagnosed with digestive cancers undergoing chemotherapy (DCUC) (colon, rectum, stomach) aged 40 to 77 years old. In the control group, blood was obtained from 21 clinically healthy male subjects, aged 35 to 75 years old. The study was approved by the Ethics Committees of the Grigore T. Popa University of Medicine and Pharmacy and of the Sf. Spiridon Emergency County Hospital of Iaşi.

Chemotherapy consisted in a combination of two drugs: an alkylating agent (Oxaliplatin) and a DNA replication inhibiting agent (oral or intravenous 5-Fluorouracil).[32]

Fresh blood was collected in 10 mM Na4EDTA tubes and used within 6 hours. An automatic analyzer ABXP60-EN (Horiba ABX, Montpellier, France) was used for blood counts, and the Auto Analyzer Slim (SEAC), W7 MIDC, Parbhani, Maharashtra) was employed for serum biochemistry. Plasma and buffy coat were separated from cells after a 15-minute centrifugation at 1500g The cells were washed three times in 10 volumes of 150 mM NaCl, 5 mM Na phosphate.[26,27]

2. Blood biochemical parameters

The clinical parameters taken into account were age and number of chemotherapy cycles over the last 5 months (CTH number). We chose beforehand the blood parameters potentially related to the hematological toxicity induced by chemotherapy, namely the red blood cells (RBC), hematocrit (HTC), hemoglobin (Hb), platelets (PL), leucocytes and lymphocytes, as well as the biochemical blood serum parameters (all of them determined in the clinical Laboratory using Automatic Analyzers as mentioned previously) that could be correlated with changes in membrane erythrocyte composition (total cholesterol and triglycerides).

Pathological hyper-triglyceridemia or hyper-cholesterolemia could constitute cancer comorbidities and are also commonly found in patients with cardiovascular diseases. In our series, the control group and DCUC groups presented normal values for total plasma cholesterol and triglycerides. We found no clinical signs or symptoms such as high blood pressure or obesity (quantified by Body Mass Index, BMI) to suggest that any of our patients had a lipid-related cardiovascular or metabolic disorder at the time they were included in the study.[33,34]

3. FTIR measurements and spectral analysis

A diluted solution of washed erythrocytes in distilled water (1:19, v/v) was prepared. Then, 5 μL from this solution was deposited on a Thallium Bromoiodine crystal and dried in vacuum (5 mm Hg at 20˚C) to remove the solvent. The mid-IR spectra were recorded in transmission with a Bruker Vertex 70 FTIR spectrometer (Bruker Optics, Germany). Each sample was analyzed in triplicate, with three spots per run, thus resulting nine spectra per each RBC sample. The signal-to-noise ratio was improved by accumulating 128 spectra with a resolution of 2.0 cm^{-1}. The preliminary spectra manipulation (eliminating the water vapors and carbon dioxide absorptions) and the data analysis were performed by means of the OPUS 6.5 software (Bruker Optics, Germany). The spectral regions of interest, used for determining the spectral parameters, were baseline-corrected by using the interactive concave rubber band method, using the same parameters for all the data. In order to minimize the influence of the baseline correction on the peak positions, two end-points of the spectral window were connected to obtain a linear baseline, which was subsequently subtracted. The peaks positions were determined with the center of gravity algorithm of the OPUS 6.5 software. The bands integrated intensity was used for determining the spectral parameters, in accordance with the known methods used in FTIR spectral analysis.[24–31] With the purpose of extracting the accurate value of the absorption bands parameters, the regions of interest of the original spectra were subjected to spectral decomposition by a multiple peak curve fitting procedure. The mixed Gaussian-Lorentzian functions and the Levenberg–Marquardt algorithm were used. The exact sub-bands position and their estimated number were determined using the second derivative spectrum and the Savitzky-Golay algorithm with a nine-point smoothing factor. In the curve-fitting procedure, the peak position was maintained fixed and the intensity, shape and width were considered as variable parameters. Such procedure was applied to the 3150 – 2750, 1750 – 1450 and 1480 – 1420 cm^{-1} domains, from where the following ratios were determined:

$\nu(=CH)/\nu_{as}(CH_3)$, $\nu_{as}(CH_2)/\nu_{as}(CH_3)$, $\delta_{sciss}(CH_2)/\delta_{as}(CH_3)$ and $\nu_{as}(CH_2)/\nu(=CH)$.

4. Statistical analysis

The Kolmogorov-Smirnov test, with the confidence level $\alpha = 0.05$, was used to test the normality of absorbance distribution for every case study group. Pearson correlation and significance of correlation, the independent Student's t-test for comparing the independent variables and the Kolmogorov-Smirnov test were performed using the SPSS® v11.0 statistical analysis package (SPSS Inc., USA). The data are presented as mean ± standard deviation (S.D.). P-values < 0.05 were considered statistically significant. The Principal Component Analysis (PCA), employed to assess the major biochemical differences, was performed using the Unscrambler X® software (Camo, Norway). The spectra in the whole range were baseline-corrected and then normalized for equal areas, using the 1170 cm^{-1} band as reference. For the PCA in the small spectral regions, the original spectra were truncated in the regions of interest: 3100 – 2750, 1770 – 1430, 1480 – 1420 and 1370 – 1000 cm^{-1}. Afterwards, these spectra were baseline-corrected using two spectral end-points and area normalized. The outlier samples were removed.

RESULTS AND DISCUSSION

1. Infrared spectral analysis

In Fig. 1 are presented the average FTIR spectra and their standard deviation (shaded areas) from control erythrocytes compared to those from DCUC group, in the spectral windows assigned to OH/NH/CH stretching vibrations (a) and fingerprint zone (b). The difference spectrum between the pathological and normal samples is given on top of each figure, to show the location of major differences. For an intact erythrocyte, the FTIR spectrum is seen as a superposition of many signals arising from a large number of components. When compared the signals of a ghost and of pure hemoglobin with those of the whole erythrocyte, it has been observed that some of the membrane vibrations of an intact erythrocyte are overlapped by those of the protein part, mainly hemoglobin.[29] In the C-H stretching region the absorptions come from both hemoglobin and membrane and are given by $\nu_{as}(CH_3)$ (2960 cm^{-1}), $\nu_{as}(CH_2)$ (2933 cm^{-1}) and $\nu_s(CH_3)$ (2870 cm^{-1}).[26,27,29] The methylene vibrations of the fatty acid chains of phospholipids appear as shoulders of these bands, around 2920 cm^{-1} ($\nu_{as}(CH_2)$) and 2850 cm^{-1} ($\nu_s(CH_2)$).[28-30]

The common feature for all cancer subjects' spectra was the wider absorption bands as compared to controls, also resulting in the loss of fine features in their second derivatives. In addition, no major differences between the spectra of the subjects receiving chemotherapy and those of recently diagnosed patients could be associated with the action of the anticancer drugs. The main indicator of the acyl chains unsaturation is $\nu(=CH)$[26-30] that usually peaks around 3012 cm^{-1}, but it is unresolved in the intact erythrocytes spectrum. These signals are accompanied in the deformation CH region by several bands given by the scissoring CH_2 (1472-1468 cm^{-1}) and bending CH_3 vibrations (1456 cm^{-1}) of the fatty acid chains.[28-30] The vibrations attributed to phospholipids polar heads are observed through the $\nu_{as}(PO_2^-)$ band at 1244 cm^{-1}, and $\nu_s(PO_2^-)$ at 1084 cm^{-1}.[26,27] The protein component is reflected by the very intense amide bands: amide I ($\nu(C=O) + \nu(C-N) + \delta(C-C-N)$, 1655 cm^{-1}) and amide II ($\nu(N-H) + \nu(C-N)$, 1543 cm^{-1}).[26,27]

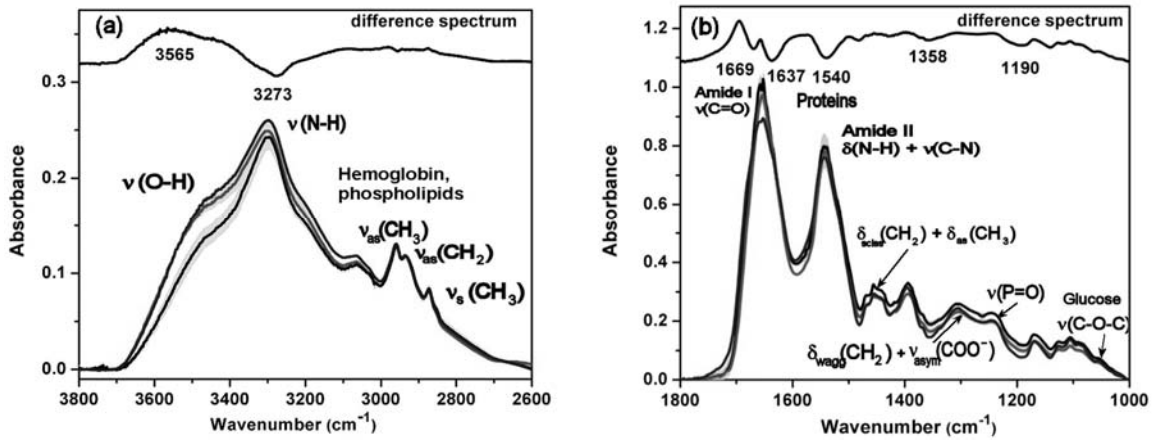

Fig. 1 – Comparison of the scale-expanded spectra of the CH and OH stretching (a) and fingerprint (b) vibrations regions for the average of representative controls (black line), new cancer patients (blue line) and cancer patients under chemotherapy (red line). Bottom: the FTIR spectra; top: the difference spectrum obtained by subtracting the average spectrum of control erythrocytes from that of abnormal erythrocytes exposed to anti-cancer drugs. The shaded areas indicate the standard deviation of the means.

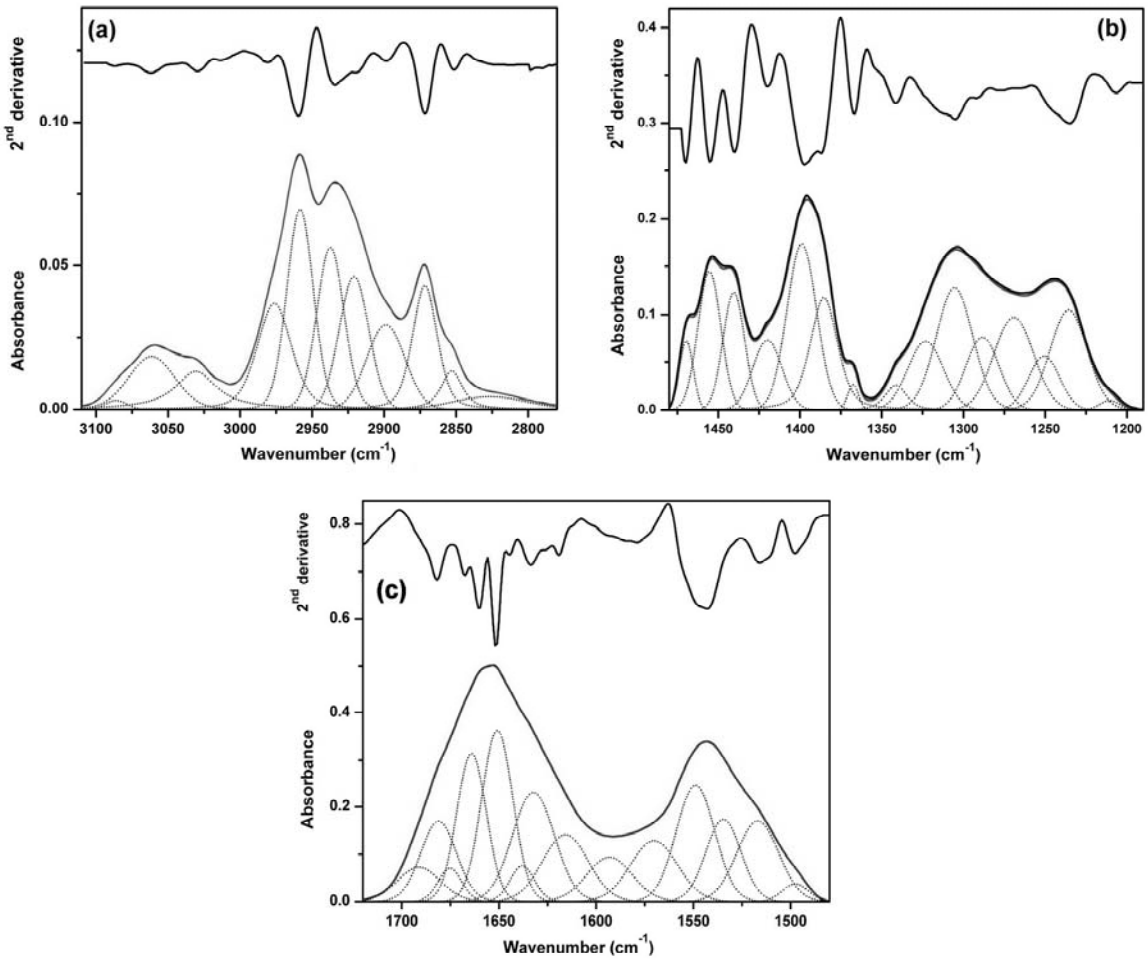

Fig. 2 – The curve – fitted regions of the FTIR spectra in the CH stretching (a), CH scissoring (b), and Amide I/II (c) vibrations domains exemplified for the control group. The second derivative spectrum is added on the top of the figure for a better comparison of the overlapped sub-bands. The red contour is the curve fitted spectrum, while the original spectrum is drawn with black line.

The Amide I and II bands are an envelope for the components characteristic to various secondary structures of polypeptide chains of proteins. Because the erythrocytes protein part is principally composed of hemoglobin (≈ 80%), the spectrin amount is almost 10%, and the others in a minor amount, it can be considered that the IR spectral analysis detects the structural changes especially in the hemoglobin conformations and in a lesser extent those in the other erythrocyte proteins.[24] For the control group, the center of gravity of the amide I band is found at 1656 cm^{-1}, consistent with the dominant α-helix structure of hemoglobin. For the DCUC group, the amide I band remained in the same position as compared to the control's, only the bandwidth value slightly increased from 61 cm^{-1} to 67 cm^{-1}.

In the regions of interest, separation of overlapped components was performed by using a combination of second derivative analysis and curve fitting procedure. The original spectra were curve-fitted using the peaks positions and intensities, estimated through the second derivative.[35,36] The results of the curve fitting process exemplified for the control group are presented in Fig. 2, for three narrow regions: the CH stretching (a), CH_2 scissoring (b) and Amide I and Amide II (c) vibrations. The curve-fitted regions of the averaged cancer group are shown in Fig. S1 (ESI).

The polyunsaturated phospholipids bearing more than four double bonds in their chain are especially susceptible to be damaged[28], so the stretching mode of the =CH group is used to monitor the unsaturation level of the lipid chains.[26-30] The evolution of the C=C bonds in the hydrophobic part of the fatty acid chains can be estimated by using the ratio of the integrated intensity of the ν(=CH) band (3020-3007 cm^{-1}) to that of $\nu_{as}(CH_3)$ (2972-2948 cm^{-1}).[26,27] The

decrease in the methylene groups amount has been evaluated by determining two parameters: the $\nu_{as}(CH_2)/\nu_{as}(CH_3)$ ratio[26,27] ($\nu_{as}(CH_2)$ integrated between 2922 and 2908 cm^{-1}), and $\delta_{sciss}(CH_2)/\delta_{as}(CH_3)$[31] ($\delta_{sciss}(CH_2)$ integrated between 1480 – 1460 cm^{-1}, and $\delta_{as}(CH_3)$, between 1460 – 1447 cm^{-1}). The value of each spectral parameter was calculated as the average of the data belonging to every case study (control and digestive cancer), extracted from the curve – fitted data of the original spectra. The plots in Fig. 3 show the differences of the spectral parameters between the two groups, which were statistically significant ($p < 0.05$).

The main features in the difference spectra between the cancer and the control group are related to variations in the secondary structures of erythrocyte proteins (the dominant protein being the hemoglobin), as seen by the negative bands around 1669 and 1637 cm^{-1}, respectively (Fig. 2 (b) and Fig. S1 (b)). The intensity differences between cancer and control related with the membrane structure are less obvious. In this case, the methylene stretching and deformation modes are especially useful to monitor the membrane structure. Therefore, it was observed that the relative amount of CH_2 moieties in the fatty acid chains, as evaluated by the $\nu_{as}(CH_2)/\nu_{as}(CH_3)$ ratio, is smaller in pathological cases as compared to the control group (Fig. 3 (a)). The relative amount of C=C bonds, given by the $\nu(=CH)/\nu_{as}(CH_3)$ ratio, shows slightly higher values for DCUC ($p < 0.01$) than for controls. The $\nu_{as}(CH_2)/\nu(=CH)$ ratio, as an analogue to the saturation index, slightly decreased for the case study ($p = 0.05$) (Fig. 3 (b)). These changes suggest an increase in the unsaturation degree of plasmatic membrane in the group of patients with cancer, which has been ascribed to the fatty acyl chain peroxidation.[26-28]

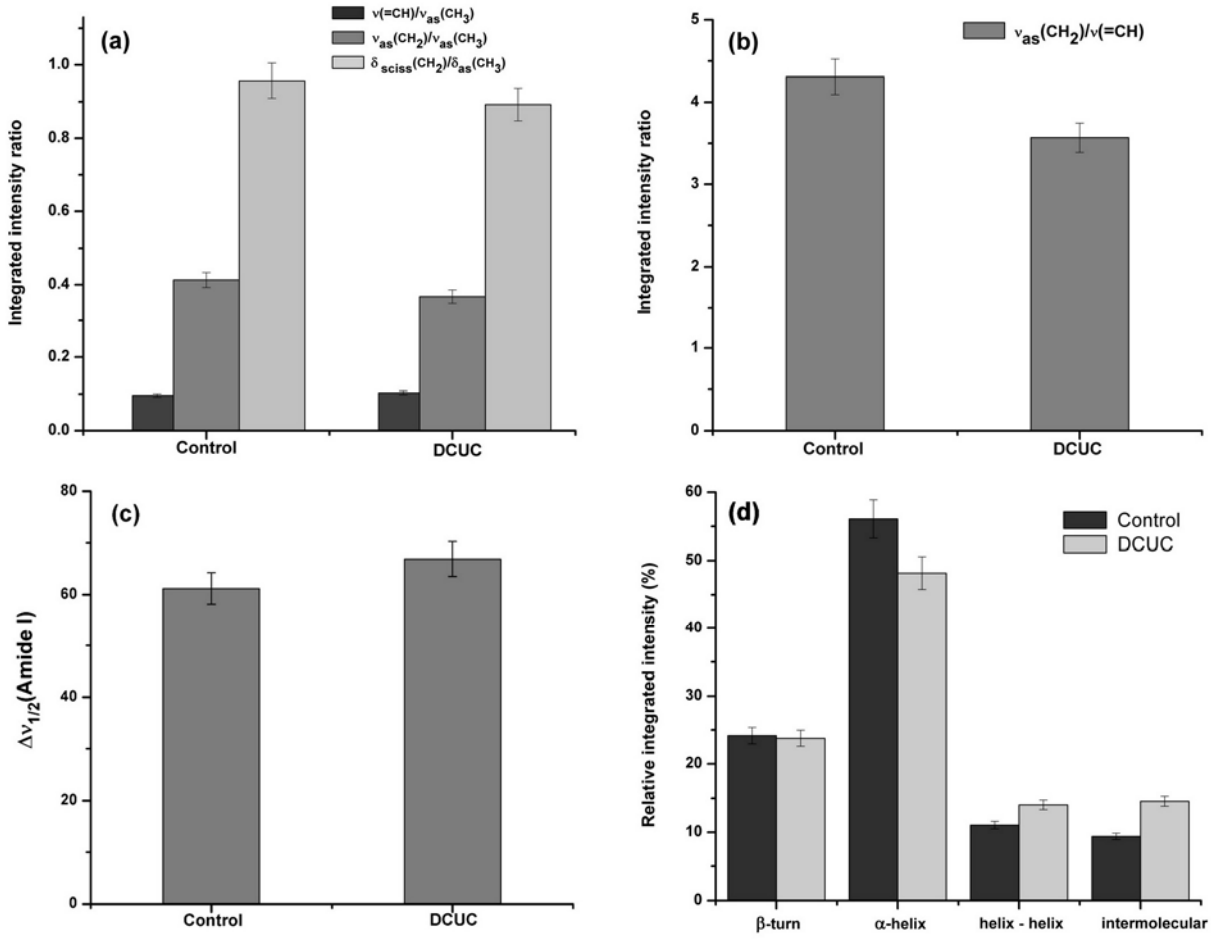

Fig. 3 – Comparison of several representative infrared spectral parameters between cancer subjects and control group: (a) $\nu(=CH)/\nu_{as}(CH_3)$, $\nu_{as}(CH_2)/\nu_{as}(CH_3)$ and $\delta_{sciss}(CH_2)/\delta_{as}(CH_3)$ ratios; (b) $\nu_{as}(CH_2)/\nu(=CH)$ ratio, as the saturation index; (c) the bandwidth of the amide I band; (d) relative proportion of the secondary structures in the protein part of erythrocytes (principally hemoglobin).

Concerning the secondary structures of the protein part, the major constituent (≈ 56%) is the α-helix conformation, whose spectral region is 1660 – 1650 cm^{-1}.[37,38] It is identified by the two underneath bands seen in the control spectra at 1663 and 1651 cm^{-1} (Fig. 2 (c)) and in the DCUC spectra at 1664 and 1651 cm^{-1} (Fig. S2 (c)). The component at 1680 cm^{-1} for control group and 1683 cm^{-1} for DCUC group may be given by β-turn structures or extended structures analogous to β-sheets.[36,37] The sub-band at 1633/1631 cm^{-1} is connected to the helix – helix interaction,[39] while that at 1619 cm^{-1} arises from intermolecular aggregates[40] and interactions between various subunits.[39] The relative proportion of the identified conformations (percentage of a given component area from the total area of the amide I band) for the control and DCUC groups is given in Fig. 3 (d). The plot indicates the high α-helical character of the protein part of erythrocyte in both cases. In the case of hemoglobin, the percentage of the α-helix structure determined by FTIR spectroscopy is lower (53%[37] to 78%[35]) than that obtained by X-ray crystallographic studies (which is 75 – 85%).[36] Because we analyzed the whole erythrocyte, the fraction of the α-helix is also lower, but close enough to other reports[37] and it may contain the secondary structures from the rest of the erythrocyte proteins.

2. Physiological parameters and correlation with the spectral parameters

The metabolic changes of erythrocytes as a function of treatment are difficult to observe, even when the second derivative spectra are analyzed, as presented in Fig. S2, ESI. When trying to correlate the IR marker bands with the number of chemotherapy cycles, only a few of them seem to be influenced at molecular level markedly enough to be visible in the FTIR spectrum. The influence of anticancer drugs on the erythrocyte constituents, extended over several chemotherapy cycles, was extracted from the FTIR parameters used in the above spectral analysis. For this, the averaged spectra of untreated subjects were subtracted from those receiving chemotherapy (CTH) (Fig. S2, ESI).

The results showing the hematological toxicity are given in Fig. 4 (a) as variations with the number of chemotherapy cycles of the $\nu_{as}(CH_2)/\nu_{as}(CH_3)$ ratio (expression of the relative content of CH_2 moieties in the fatty acid chains).[34,35] The data in Fig. 4 (b) show the evolution of the position of the symmetric stretching vibration of methylene groups and of the relative number of the C=C bonds.

The chemotherapeutic treatment induced a progressive increase of the number of methylene groups, while the extent of alteration in the case of protein component appears to be less dramatic (Fig. 4 (a)). In turn, the inverse relationship between $\nu_{as}(CH2)/\nu_{as}(CH_3)$ and $\nu(=CH)/\nu_{as}(CH_3)$ is no longer available (Fig. 4 (b)). The drug's response of the $\nu_{sym}(CH_2)$ of the membrane phospholipids seems then to be an increased conformational order of the acyl chains, observed through the shift of the $\nu_{sym}(CH_2)$ frequency towards lower values. However, the frequency variation is very small (lower than 1 cm^{-1}) and the decrease stopped to the end of the 5th cycle and increases again at the end of the monitored treatment period. When confronted with the relative number of CH_2 groups in the acyl chains in the 6-th cycle, it is reasonable to link the lower saturation degree (low $\nu_{as}(CH_2)/\nu_{as}(CH_3)$ value) with the higher frequency, which means an increase in conformational disorder and a higher chain flexibility. The impact of cytostatics on the erythrocyte's components displays a cyclic evolution, observed from the difference spectra displayed in Fig. S2. Turning into spectral parameters, the unsaturation degree of the membrane fatty acid chains increased during the first four cycles of chemotherapy (Fig. 4 (a)). This evolution time frame is almost equivalent to the erythrocyte life period, which is around 120 days. Therefore, the variations in the erythrocyte's chemistry seem to be related to the regenerating period of these cells.

The hematological, serum and spectral parameters of the healthy and cancer patients receiving chemotherapy, listed in Table S1 (ESI), were compared by the Student's t-test and the results are presented in Table S2 (ESI). It is observed that the $\nu_{as}(CH_2)/\nu_{as}(CH_3)$ ratio showed a direct and medium-strength correlation with the number of chemotherapy cycles ($p = 0.04$). Also, $\nu_{as}(CH_2)/\nu_{as}(CH_3)$ is strongly correlated with HCT ($p > 0.05$), glucose level ($p > 0.05$) and lymphocyte values ($p > 0.05$). The saturation degree of the fatty acids associated with the $\nu(=CH)/\nu_{as}(CH_3)$ ratio shows medium correlations with the number of chemotherapy cycles, total cholesterol level, triglycerides, WBC, lymphocytes and Hb ($p > 0.05$).

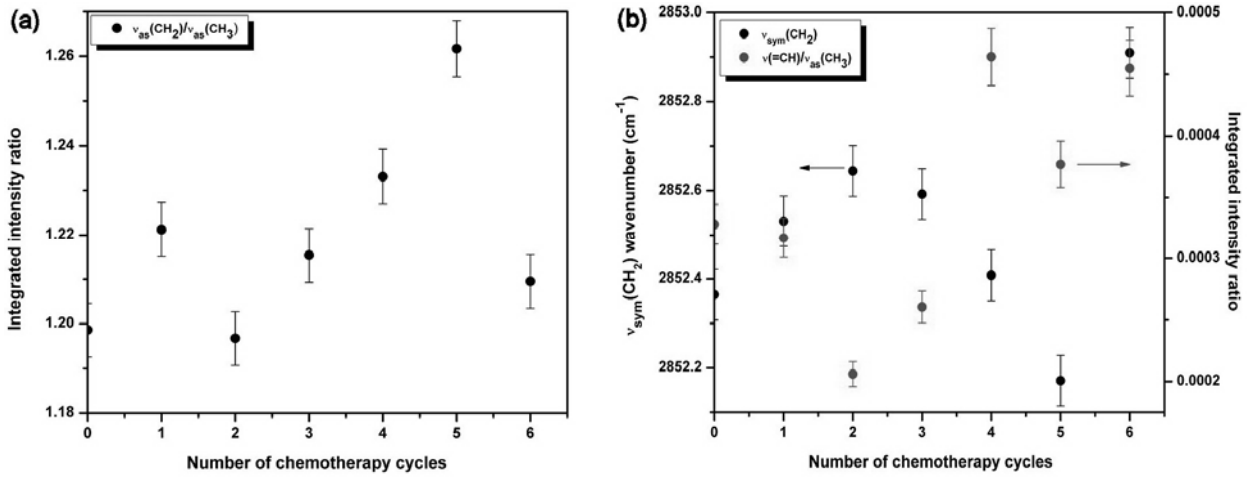

Fig. 4 – Evolution of several spectral parameters with chemotherapy: (a) the relative number of methylene groups in the fatty acid chains, expressed as the $\nu_{as}(CH_2)/\nu_{as}(CH_3)$ ratio; (b) the relative number of C=C bonds in acyl chains ($\nu(=CH)/\nu_{as}(CH_3)$), and the wavenumber of $\nu_{sym}(CH_2)$, related with the conformational order of the same chains.

The inverse correlation between the relative number methylene and C=C groups in the acyl chains seems to be broken when the influence of the chemotherapy is discussed (Fig. 4 (b)). The explanation could be the drug penetration and propagation route through the membrane bilayers, and its final location among the bilayer components. The asymmetric distribution of phospholipids across the erythrocyte membrane and their variety constitute another aspect to consider. This cooperative change in the hydrophobic part of the membrane may also indicate interference with other processes of unknown origin, occurring during the chemotherapeutic treatment.

3. Principal Component Analysis (PCA)

The scatter plots of principal component 1 (PC-1) against PC-2 for the CH stretching region is presented in Fig. 5, altogether with the comparative view of the normalized spectra for the case studies and the loading plots. PC-1 explains 89% of the total variance (in brackets in the figure 5), and PC-2 has 9% variability. The minor differences between the spectra (Fig. 5 (a)) were better discriminated by PCA analysis, which provided satisfactory data segregation (Fig. 5 (b)). The erythrocytes from the normal samples are clustered mostly in the first quadrant, where the values of both PC-1 and PC-2 are positive, while the cancer case studies are scattered over the other three quadrants, mainly in the negative direction of PC-1. The loading plot of PC-1 (Fig. 5 (c)) has negative correlations at 3062, 2960, 2926 and 2870 cm^{-1}, which correspond to amide B band and stretching vibrations of CH_2 and CH_3 groups, respectively. In the negative loading of PC-2, $\nu_{as}(CH_3)$ (2980 cm^{-1}) and $\nu_s(CH_3)$ (2970 cm^{-1}) contribute to variance. These fundamental modes belong essentially to the membrane phospholipids, with a minor contribution from hemoglobin[34,35,37]; $\nu_{as}(CH_2)$ around 2926 cm^{-1} is given by the fatty acid chains. Therefore, it seems that the greatest degree of variance in the CH stretching zone is given by the changes in the chemical structure of the membrane, and in a minor amount from hemoglobin.

The PCA run in the amide I and II region also discriminates the control and abnormal samples, as shown in Fig. 6. In the comparative picture of the amide I and II bands superposed for the two cases analyzed (Fig. 6 (a)), the amide I band of abnormal samples is slightly wider and with a lower intensity than that of the control group.

The spectral segregation in two clusters is presented in Fig. 6 (b). The spots of cancer cases are spread mainly in the negative directions of PC-1 and PC-2, while the normal samples are grouped along the positive direction of PC-1, in the first two quadrants. Eighty-four percent of the variance is explained by PC-1 and its loading plot is dominated by two negative bands at 1655 and at 1544 cm^{-1}. The first peak originates from the α-helix component of the amide I band, while the second, from the amide II band. The positive feature at 1692 cm^{-1} might be given by intramolecular aggregates of hemoglobin.[40] In the loading plot of PC-2, the negative peak at 1655 cm^{-1} is enclosed between one negative (1696 cm^{-1}) and one positive peak (1633 cm^{-1}). These two side peaks arise from the C=O vibration of intramolecular aggregates and the short sequences

linking the helical units, respectively. The broadening of the amide I band for the DCUC group with no obvious shift of the maximum can be explained by the increased contribution of those carbonyl groups belonging to interacting α-helices and those located in aggregates. This increase is made at the expenses of the slightly reduction of the α-helix amount. In addition, it is apparent that the protein chains develop some irregular and unfolded structures, seen in the growing of the weak band around 1692 cm^{-1}.

PCA can be extended to other spectral regions, such as those including the methylene group vibrations in the bending region (Fig. S4) or the phosphate group vibrations (Fig. S5). The loading plots indicate those bands responsible for the differences obtained through the discrimination procedure.

These preliminary results show that the effects of cancer and chemotherapy on erythrocytes are oxidative stresslike, although not all the infrared spectral parameters reported in literature to be sensitive to this process were observed to change in our study. The tolerability and health-related quality of life is influenced by the administrated dose, taking into consideration the efficacy and the general systemic effects like anemia. While TDM could involve high costs, the erythrocyte FTIR analyses will not imply important expenses. This method uses routine blood samples; no special experimental conditions or special agents are necessary and may have clinical implication by anticipating the hematologic toxic effect of the chemotherapy.

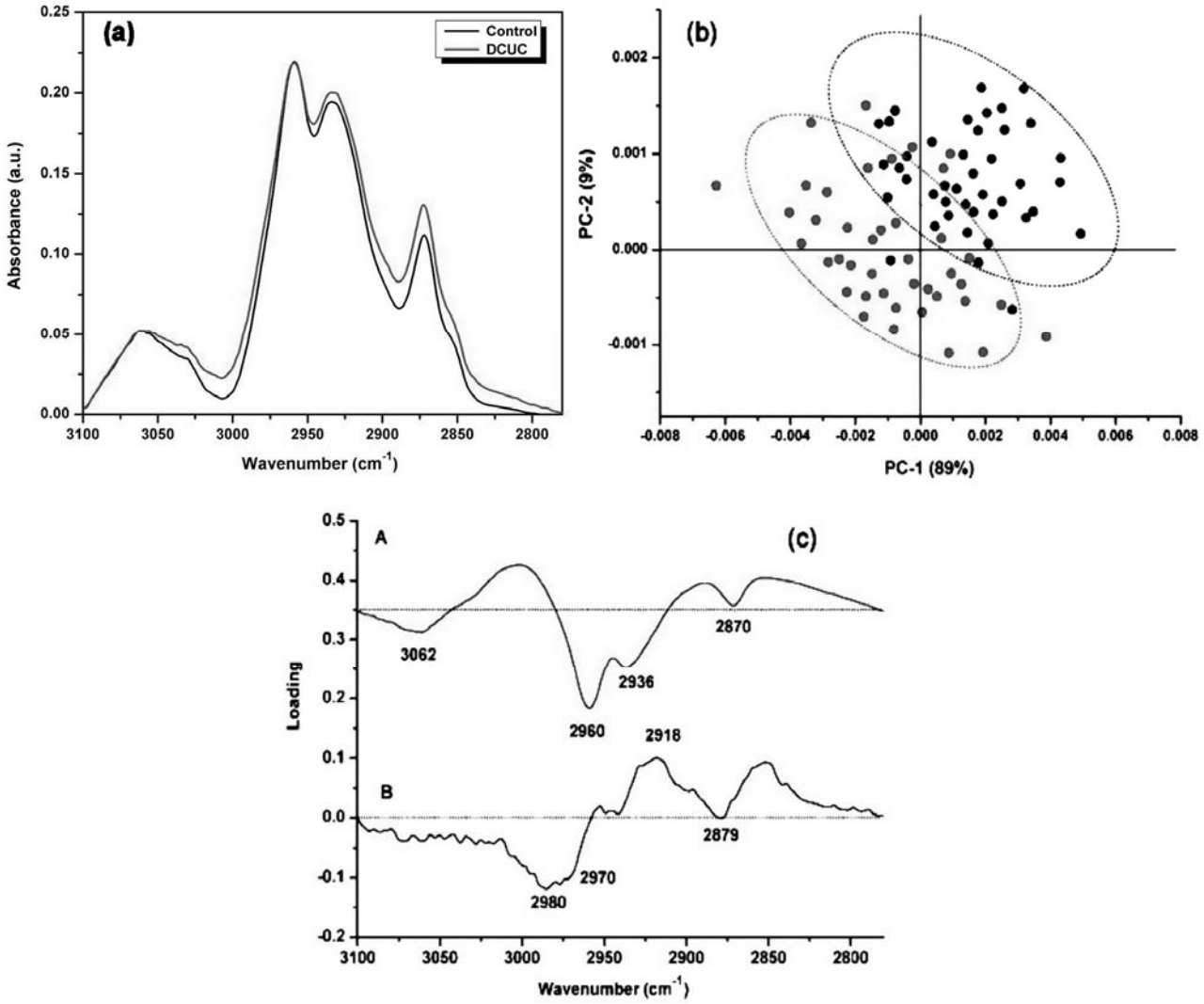

Fig. 5 – (a) FTIR spectra of erythrocytes in the CH stretching region for the control samples as compared to those from the cancer cases. The spectra were normalized with respect to $\nu_{as}(CH_3)$ (2980 cm^{-1}). (b) The scores plots on the two PCs: black trace – normal samples, red trace – abnormal samples. The percentages in brackets represent the contribution of each PC to the total variance. The ellipses delimitate the samples clustering. (c) Loading plots of PC-1 (A) and PC-2 (B).

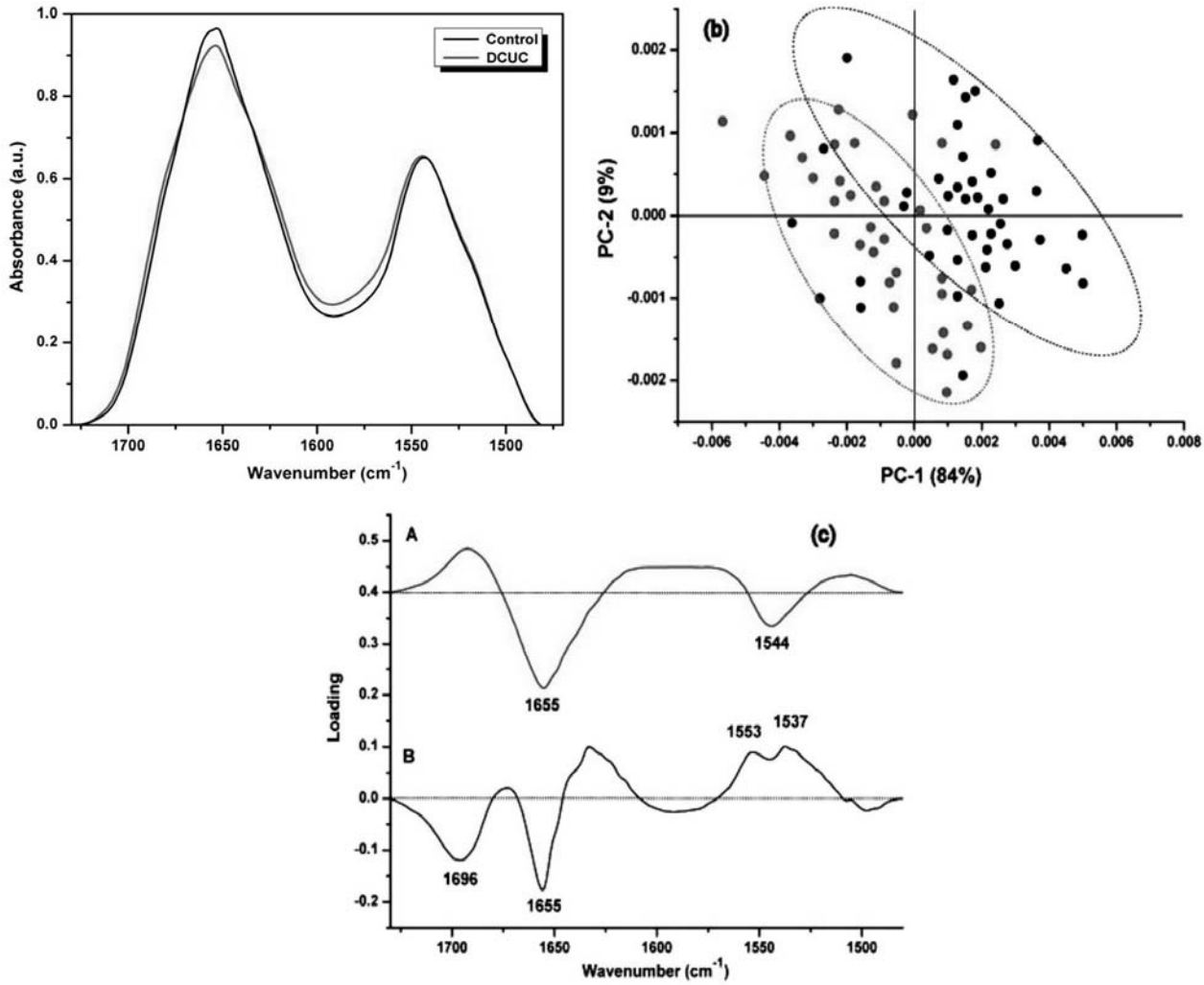

Fig. 6 – (a) FTIR spectra of erythrocytes in the amide I and II region for the control samples as compared to those from the cancer cases. The spectra were normalized with respect to the amide II band, for a better visualization. (b) Scatter plots on the two PCs: black trace – normal samples, red trace – abnormal samples. The ellipses delimitate the samples clustering. (c) Loading plots of PC-1 (A) and PC-2 (B).

CONCLUSION

A FTIR spectroscopy/PCA analysis was applied to characterize and differentiate the erythrocytes from healthy individuals and digestive cancer subjects under chemotherapy. The spectral analysis suggested characteristic patterns for the abnormal erythrocytes, as both the membrane and the hemoglobin suffered changes in their chemical structure. PCA may provide even more insight into the specific structural differences between the two kinds of erythrocytes, revealing changes in the molecular structure of the membrane lipids and variations in the content of some secondary structures of hemoglobin. The putative utility of this study could be related to the development of an accurate, reliable and cost-saving analytical technique for toxic effects of chemotherapy on the erythrocyte.

REFERENCES

1. C. B Wood, N. A. Habib, A. Thompson, H. Bradpiece, C. Smadja, M. Hershman, W. Barker and K. Apostolov, *Br. Med. J. (Clin. Res. Ed.)*, **1985**, *291*, 163-165.
2. K. Kuriki, K. Hirose, K.Wakai, K. Matsuo, H. Ito, T. Suzuki, A. Hiraki, T. Saito, H. Iwata, M. Tatematsu and K. Tajima, *Int. J. Cancer,* **2007**, *121*, 377-385.
3. K. Kuriki, K.Wakai, K. Hirose, K. Matsuo, H. Ito, T. Suzuki, T. Saito, Y. Kanemitsu, T. Hirai, T. Kato, M. Tatematsu and K. Tajima, *Cancer Epidemiol. Biomarkers Prev.*, **2006**, *15*, 1791-1798.
4. R. B. Harris, J. A. Foote, I. A. Hakim, D. L. Bronson and D. S. Alberts, *Cancer Epidemiol. Biomarkers Prev*., **2005**, *14,* 906-912 .
5. S. Croci, I. Ortalli, G. Pedrazzi, G. Passeri and P. Piccolo, *Hyperfine Interactions,* **2000**, *126*, 47-52 .
6. G. Mantovani, A. Maccio, C. Madeddu, L. Mura, G. Gramignano, M. R. Lusso, C. Mulas, M. C. Mudu, V. Murgia, P. Camboni, E. Massa, L. Ferreli, P. Contu, A. Rinaldi, E. Sanjust, D. Atzei and B. Elsener, *Int. J. Cancer*, **2002**, *98*, 84-91.

7. K. Kolanjiappan, S. Manoharan and M. Kayalvizhi, *Clin. Chim. Acta*, **2002**, *326*, 143-149.
8. M. Khanmohammadi, F. H. Rajabi, A. B. Garmarudi and R. Mohammadzadeh, *Eur. J. Cancer Care (Engl)*, **2010**, *19*, 352-359.
9. A. M. Florea and D. Busselberg, *Cancers*, **2011**, *3*, 1351-1371.
10. M. Gago-Dominguez, J. E. Castelao, M. C. Pike, A. Sevanian and R. W. Haile, *Cancer Epidemiol. Biomarkers Prev.*, **2005,** *14,* 2829-2839.
11. J. M. Gutteridgea and B.Halliwell, *Trends Biochem. Sci.,* **1990**, *15* , 129-135.
12. B. S. Thomas, J. O'Dea and I. S. E Fentiman, *Br. J. Surg.*, **1988**, *75*, 1078-1079.
13. C. Crespi, S. Quevedo, P. Roca and A. Palou, *IUBMB Life,* **1999,** *48*, 531-537.
14. J. P. Neoptolemos and B. S. Thomas, *Ann. Clin. Biochem*., **1990**, *27*, 38-43.
15. M. Pandey, L. B. Sharma, S. Singh and V. K. Shukla, *World J. Surg. Oncol.,* **2003**, *1***,** 5-12.
16. M. Pandey, A. K. Khatri, S. S. Dubey, A. Gautam and V. K. Shukla, *J. Surg. Oncol.,* **1995**, *59* **,** 31-34.
17. M.M. Cruz Silva, V.M.C. Madeira, L.M. Almeida and J.B.A. Custódio, *Biochim. Biophys. Acta*, **2000**, *1464*, 49-61.
18. M.M. Cruz Silva, V.M.C. Madeira, L.M. Almeida and J.B.A. Custódio, *Toxicology in Vitro*, **2001**, *15*, 615–622 .
19. A. Marczak, A. Kowalczyk, A. Wrzesien-Kus, T. Robak and Z. Jozwiak, *Cell Biol. Int.*, **2006**, *30* **,** 127-132.
20. E. Gamelin, A. L. Bouil, M. Boisdron-Celle, A. Turcant, R. Delva, A. Cailleux, A. Krikorian, S. Brienza, E. Cvitkovic, J. Robert, F. Larra and P. Allain, *Clin. Cancer Res.,* 1**997**, *3* , 891-899.
21. R. Mandal, M. B. Sawyer and X. F. Li, *Rapid Commun. Mass. Spectrom.*, **2006**, *20* , 2533-2538.
22. I. Spasojevic, S. Jelic, J. Zakrzewska and G. Bacic, *Molecules*, **2009**, 1*4* , 53-67.
23. G. M. Baerlocher, J. H. Beer, G. R. Owen, H. J. Meiselma, W. H. Reinhart, *Br. J. Haematol.,* **1997**, *99*, 426-432 .
24. A. Dong, R.G. Messerschmidt and J. A. Reffner, *Biochem. Biophys. Res. Commun*., **1988,** *156* , 752-756.
25. A. Dong and W. S. Caughey, "Infrared methods for study of hemoglobin reactions and structures", in "Methods in enzymology", vol. 232, Academic Press, New York, 1994, p. 139 - 175.
26. C. Petibois and G. Deleris, *Analyst,* **2004**, *129* , 912-916.
27. C. Petibois and G. Deleris, *Cell Biol. Intl.*, **2005**, *29*, 709-716.
28. R. H. Sills, D. J. Moore and R. Mendelsohn, *Anal. Biochem.*, **1994**, *218 ,* 118-123.
29. D.J. Moore, R.H. Sills and R. Mendelsohn, *Biospectroscopy*, **1995**, *1* , 133-140.
30. D. J. Moore, S. Gioioso, R. H. Sills and R. Mendelsohn, *Biochim. Biophys. Acta A - Biomembrane*, **1999**, *1415*, 342-348.
31. K.-Z. Liu, M. Jackson, M.G. Sowa, H. Ju, I.M.C. Dixon and H.H. Mantsch, *Biochim. Biophys. Acta,* 1**996**,*13*, 173-177.
32. G. Goel, M. Jauhri, A. Negi and S. Aggarwal, *Hematol. Oncol. Stem Cell. Ther*., **2010**, *3* , 55-59.
33. L. Berglund, J. D. Brunzell, A. C. Goldberg, I. J. Goldberg, F. Sacks, M. H. Murad and A. F. Stalenhoef, *J. Clin. Endocrinol. Metab.*, **2012**, *97* , 2969-2989.
34. E. Braunwald and R. O. Bonow. "Principles in drug teraphy" in "Braunwald's heart disease: a textbook of cardiovascular medicine" , 9th edn., Saunders, Philadelphia , 2011, p. 91-99.
35. A. Dong, P. Huang and W. Caughey, *Biochemistry*, **1990**, *29*, 3303 – 3308.
36. A. Dong, P. Huang and W. Caughey, *Arch. Biochem. Biophys.*, **1995,** *320*, 59 – 64.
37. Q. Shao, P. Wu, P. Gu, X. Xu, H. Zhang and C. Cai, *J. Phys. Chem. B*, **2011**, *115,* 8627–8637.
38. H. Cheng, H. Liu, W. Bao and G. Zou, *J. Photochem. Photobiol. B: Biology*, **2011**, *105*, 126–132.
39. O. Sire, C. Zentz, S. Pin, L. Chinsky, P.Y. Turpin, P. Martel, P.T.T. Wong and B. Alpert, *J. Am. Chem. Soc.*, **1997**, *119,* 12095 – 12099.
40. M. Mahato, P. Pal, T. Kamilya, R. Sarkar, A. Chaudhuri and G.B. Talapatra, *J. Phys. Chem. B*, **2010,** *114***,** 7062–7070.